# Electron spin resonance of the two-dimensional electron system in $Al_xGa_{1-x}As/GaAs$ at subunity filling factors

R. Meisels, I. Kulac, and F. Kuchar
*Department of Physics, University of Leoben, A-8700 Leoben, Austria*

M. Kriechbaum
*Institute for Theoretical Physics, University of Graz, A-8010 Graz, Austria*

(Received 27 April 1999)

The electron spin resonance (ESR) of a two-dimensional electron system (2DES) in $Al_xGa_{1-x}As/GaAs$ in the regime of fractional filling ($\nu<1$) of the lowest Landau level is investigated by a photoconductivity technique at millimeter wave frequencies. By performing the experiments in a standing wave the ESR is shown to be a magnetic-dipole transition. This is in agreement with a calculation based on an 8-band model and $\mathbf{k}\cdot\mathbf{p}$ theory. The (single-electron) theory also yields excellent agreement for the experimental and theoretical magnetic field dependences of the ESR transition energy, i.e., single-electron transition energies are measured and Kohn's theorem is not violated. Nevertheless, due to electron-electron interaction the ground state of the 2DES can be a many-particle state with similar amplitudes of spin-up and spin-down contributions. Evidence for such a reduced spin polarization is found in a striking reduction of the ESR strength when decreasing the temperature from 1.6 to 0.3 K.

## I. INTRODUCTION

Two-dimensional electron systems (2DES) in semiconductor heterostructures and MOS structures show a variety of interesting phenomena with $Al_xGa_{1-x}As/GaAs$ representing a prototype system for the heterostructures.[1] The 2DES in $Al_xGa_{1-x}As/GaAs$ is also of particular interest because of the small effective $g$ factor ($g^*\approx -0.4$) making spin effects of great importance. The most direct information on the spin properties can be obtained from an investigation of the conduction electron spin resonance (ESR). In a previous work,[2,3] the ESR was studied in high magnetic fields at Landau level filling factors $\geqslant 1$, i.e., in the regime of the integer quantum Hall effect (QHE). The observed ESR transition energies could be described by using a $\mathbf{k}\cdot\mathbf{p}$ calculation for independent electrons.[4] A variety of transport and optical phenomena can also be understood in the independent-electron picture. However, in several cases interaction effects have proven essential for an interpretation, e.g., of the metal-insulator transition in a 2DES at zero magnetic field[5] and of the fractional quantum Hall effect (FQHE) at high fields.[6–9] In the independent-electron approach at sufficiently high magnetic fields only the lower spin sublevel of the $N=0$ Landau level is occupied (filling factor $\nu<1$). Due to Coulomb interaction effects, however, a many-body ground state with similar amplitudes of spin-up and spin-down can exist at sufficiently low temperatures as has been shown by finite-size calculations.[10,11] The effect of the interaction can be particularly strong in semiconductors like GaAs because of the small value of the effective $g$ factor and of the Zeeman splitting ($g^*\mu_B B$). A transition from a spin-polarized to a spin-unpolarized state is predicted to occur when lowering the temperature below 1 K. Experimental evidence for spin polarizations smaller than expected from the independent electron picture has been found in measurements of the nuclear magnetic resonance[12] and of interband transitions.[13]

In the present paper, we study the ESR of the 2DES in $Al_xGa_{1-x}As/GaAs$ in high magnetic fields where the filling of the lowest Landau level is smaller than unity and at temperatures where the FQHE develops (1.6→0.3 K). Because of the small $g$ factor the experiments have to be performed at millimeter wave (MMW) frequencies of about 50 GHz. The first purpose is to investigate the mechanisms responsible for the ESR absorption and its detection as a millimeter wave (MMW) photoconductivity signal. Among other questions, this concerns the dominance of electric (EDT) or magnetic dipole transitions (MDT). The second purpose concerns the possible influence of interaction effects on the spin resonance under conditions where the FQHE is observed ($\nu<1$). These interaction effects are not included in the $\mathbf{k}\cdot\mathbf{p}$ calculations of Ref. 4 and have not been detected in previous ESR experiments.[2,3] This has been in agreement with the expections from Kohn's theorem,[14] *viz*. that in a resonance transition there is no coupling to the relative coordinates of the particles. However, Kohn's theorem is valid only for a parabolic band structure, a condition that is not strictly met by 2DES. It is therefore of interest whether the predicted ESR energy dependence on magnetic field[4] applies also at high magnetic fields in the fractional filling factor regime at $\nu<1$ where the many-body interactions that are responsible for the FQHE dominate. Even if there is no effect on the ESR energy due to Kohn's theorem, many-body effects could affect the strength of the ESR, e.g., via the relative amplitudes of the spin-up and spin-down contributions to the many-particle ground state.

## II. EXPERIMENTAL ARRANGEMENT

The experiments are performed on an $Al_{0.35}Ga_{0.65}As/GaAs$ heterostructure with [001] growth direction. The substrate has a thickness of about 0.5 mm, and

 ©2000 The American Physical Society

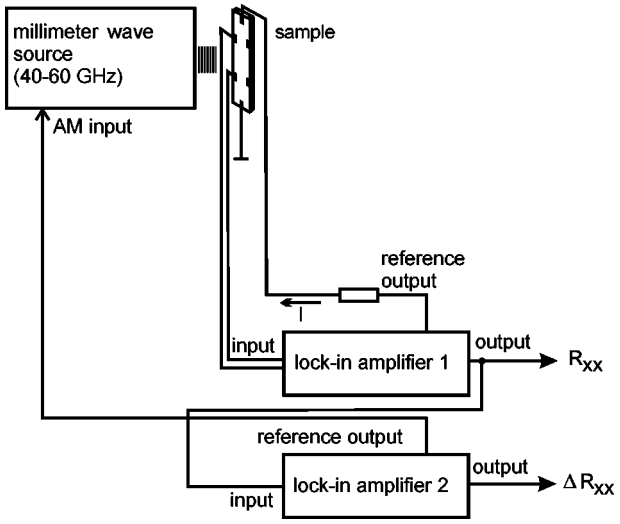


FIG. 1. Experimental arrangement for the measurement of $\Delta R_{xx}$. The longitudinal resistance $R_{xx}$ is measured by the lock-in amplifier 1. The lock-in amplifier 2 is used to detect the change of the longitudinal resistance $\Delta R_{xx}$ due to the amplitude modulated (AM) millimeter waves.

the $Al_xGa_{1-x}As$ is 78 nm thick with a 35-nm Si-doped layer separated by a 43-nm spacer from the GaAs. The GaAs cap layer has a thickness of 20 nm. The electron density is $n_s = 1.4\times10^{11}$ cm$^{-2}$ and the mobility is $\mu = 0.8 \times 10^6$ cm$^2$/Vs. The sample is 7-mm long and 3-mm wide with current and voltage contacts alloyed into the sample edges using In dots. The measurements are performed at temperatures between 1.6 and 0.3 K in magnetic fields up to 10.7 T.

The ESR absorption was too weak to be directly observable in transmission (see also Refs. 2 and 3). It can, however, be observed in photoconductivity, i.e., via the change of the longitudinal resistance $\Delta R_{xx}$ due to the absorption of the millimeter waves by the 2DES. A double lock-in technique is used to measure $R_{xx}$ and $\Delta R_{xx}$. The measuring circuit is shown in Fig. 1. A constant ac current ($f_I \approx 100$ Hz) with up to 1.5 $\mu$A rms is applied to the sample with a 10 M$\Omega$ resistor in a series. Fully modulated millimeter waves ($f_{mod} \approx 13$ Hz) in the $U$-band (40-60 GHz) are directed onto the sample by a rectangular wave guide. The power incident on the sample is about 5 mW. The first lock-in amplifier is set to the frequency $f_I$ and measures a signal proportional to $R_{xx}$. The $R_{xx}$ signal contains an oscillatory component with frequency $f_{mod}$ proportional to $\Delta R_{xx}$. In order to transfer this component without attenuation to the output the time constant is set to a low value (10 ms). The $\Delta R_{xx}$ signal is extracted by the second lock-in amplifier set to $f_{mod}$. Its time constant is large (3 s) to minimize noise.

In most of our experiments an absorber is placed behind the sample so that the measurements are performed with propagating waves. In order to investigate the dominance of electric or magnetic dipole interaction a standing wave is created by placing a short at certain distances behind the sample. Thus the sample can be placed at positions with a maximal magnetic MMW field accompanied by vanishing electric field or vice versa.

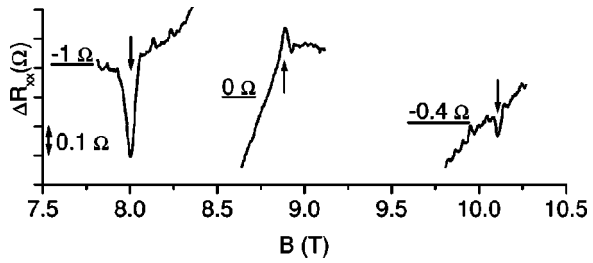


FIG. 2. Millimeter wave induced change of the longitudinal resistance $\Delta R_{xx}$ for three frequencies ($\Delta R_{xx}$ scales are shifted against each other). The ESR is marked by arrows. $T = 1.6$ K.

## III. EXPERIMENTAL RESULTS

Figure 2 shows $\Delta R_{xx}$ at 1.6 K for a range of frequencies. The ESR signal (marked by an asterisk) appears as a dip or peak on a nonresonant background. The background signal is particularly strong in magnetic field regions adjacent to the minima where $R_{xx}$ varies rapidly.[3,15] The polarity of the ESR signal coincides with the polarity of the background, i.e., there are peaks where the background is positive and dips where the background is negative. The field dependences of the ESR frequency $\omega_{ESR} = g^*\mu_B B$ and of the effective $g$ factor $g^*$ are plotted in Fig. 3. When reducing the temperature below 1.6 K the ESR shows a striking behavior. At the temperature of 1.2 K the ESR disappears in the vicinity of the fractional filling factor $\nu = 2/3$ (B=9 T) and around 8.2 T. The latter region is not associated with a particular fractional $R_{xx}$ minimum. Reducing the temperature further to 0.3 K causes a disappearance of the ESR signal in $\Delta R_{xx}$ over the full magnetic field range (7-10 T) examined. As an example, observations at 1.6 and 0.3 K are compared in Fig. 4. While the ESR disappears the strength of the background signal increases by about two orders of magnitude.

Previous work[16,17] found a dependence of the shape of the ESR signal and of the ESR position on the direction of the magnetic field sweep around odd filling factors. In the present work no such dependence is seen. Two typical traces

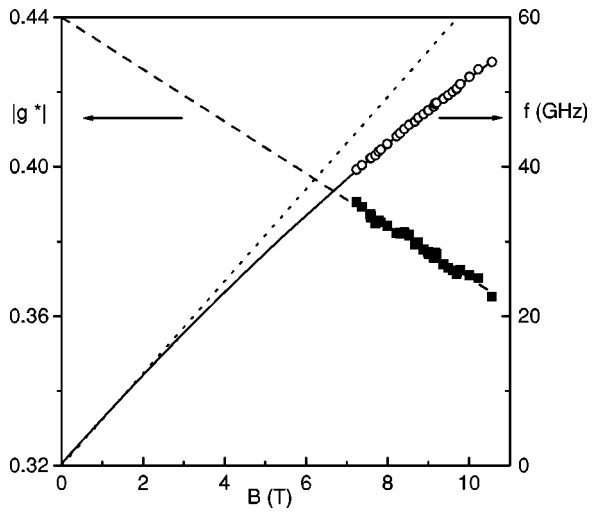


FIG. 3. Dependence of the ESR frequency and of the effective $g$ factor on the magnetic field at 1.6 K. The dotted line corresponds to a constant $g$ factor ($-0.44$). Dashed and full lines are calculations according to Eq. (4.4) and Ref. 4.

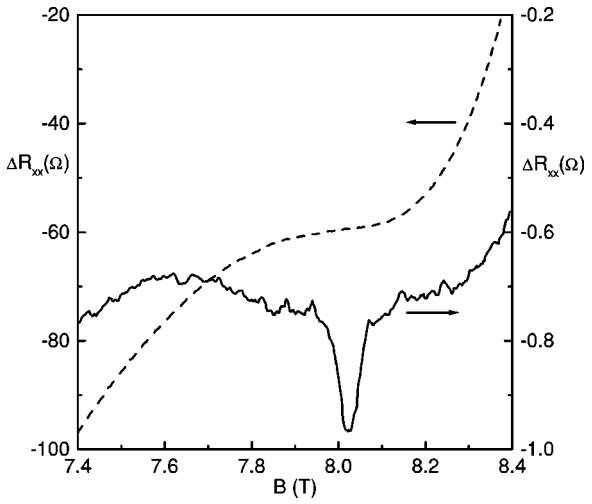


FIG. 4. $\Delta R_{xx}$ taken at 0.3 K (dashed) and at 1.6 K (solid), $f=43$ GHz.

for up and down sweeps taken at $f=43$ GHz and $T=1.6$ K are shown in Fig. 5. Also at 1.2 K the up and down sweeps give identical results within the noise level.

Figure 6 shows the ESR signal with the sample placed at different positions in the standing wave pattern in front of a reflecting short. λ/2 corresponds to a maximum of the MMW magnetic field and a node of the electric field. At λ/4 and 3λ/4 the electric field is maximal and the magnetic field minimal. The strength of the ESR correlates with the strength of the magnetic field component, i.e., the ESR is maximal at the maxima of the magnetic field and vanishes at the nodes.

## IV. THEORY

### A. Electronic band structure of the 2DES

To determine the properties of the 2DES a $\mathbf{k}\cdot\mathbf{p}$ perturbation calculation is performed using eight conduction and valence bands: the $\Gamma_6(S\uparrow,S\downarrow)$ conduction bands and the spin-orbit split $\Gamma_8,\Gamma_7$ valence bands made up of $(X,Y,Z)\times(\uparrow,\downarrow)$ states.[4,18] The contributions of higher bands ($k^2$ terms) are neglected for the electromagnetic transition-matrix elements while taken into account for the calculated energies. Then the relevant cross terms between the conduction and valence bands are[18]

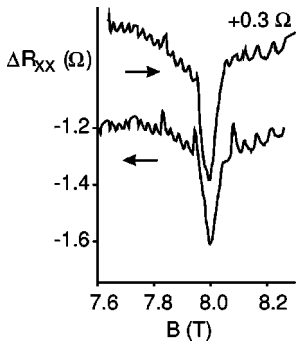


FIG. 5. $\Delta R_{xx}$ recorded with rising (top) and falling magnetic field (bottom). $f=43$ GHz, $T=1.6$ K.

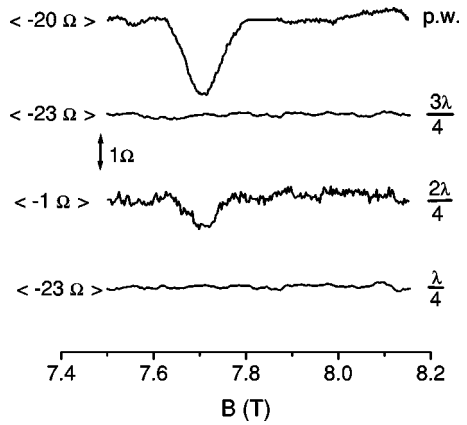


FIG. 6. Millimeter wave induced change of the longitudinal resistance $\Delta R_{xx}$ with the sample placed in the standing wave pattern in front of a short at different distances ($d=\lambda/4$, $\lambda/2$, and $3\lambda/4$). Shown is also the result for a propagating wave (p.w.). The nonresonant background was removed from the $\Delta R_{xx}$ traces. Its values are given in brackets. $f=42$ GHz, $T=1.3$ K.

$$H_{68}=\sqrt{3}[T_x(Pk_x+iC_2\epsilon_{yz})+\text{c.p.}],$$

$$H_{67}=-1/\sqrt{3}[\sigma_x(Pk_x+iC_2\epsilon_{yz})+\text{c.p.}]. \tag{4.1}$$

Here, $P$ is the interband momentum matrix element, $\epsilon_{yz}$ is the strain tensor, and $C_2$ is the appropriate interband strain deformation potential;[18] c.p. denotes cyclic permutation. The cross matrices $T$ are

$$T_x=1/(3\sqrt{2})\begin{pmatrix}-\sqrt{3} & 0 & 1 & 0\\ 0 & -1 & 0 & \sqrt{3}\end{pmatrix},$$

$$T_y=-i/(3\sqrt{2})\begin{pmatrix}\sqrt{3} & 0 & 1 & 0\\ 0 & 1 & 0 & \sqrt{3}\end{pmatrix}, \tag{4.2}$$

$$T_z=\sqrt{2}/3\begin{pmatrix}0 & 1 & 0 & 0\\ 0 & 0 & 1 & 0\end{pmatrix}.$$

The $\sigma$'s are the Pauli spin matrices.

As this paper concentrates on the conduction band, the 8×8 Hamiltonian is reduced to a 2×2 Hamiltonian perturbatively. This yields a Hamiltonian

$$H(\mathbf{k})=\sum_{\kappa,\lambda} a_{\kappa,\lambda}\sum_l X_l^{(\kappa,\lambda)}H_l^{(\kappa,\lambda)}(\mathbf{k}). \tag{4.3}$$

$\kappa$ corresponds to irreducible representions $\Gamma_\kappa$. For the 2×2 conduction-band matrix the relevant representations are $\Gamma_1$ (unit matrix) and $\Gamma_4$ (The basis of this represention is formed by the Pauli spin matrices.) Depending on $\kappa$, $l=x,y,z(\kappa=4)$ or $l=1(\kappa=1)$. In the first case, $X_l^{(4,\lambda)}=\sigma_l$, in the second case, $X_1^{(1,\lambda)}$ is the 2×2 unit matrix. The index λ further enumerates different components of the Hamiltonian, e.g., $H_1^{(1,1)}(\mathbf{k})=1$, $H_1^{(1,2)}(\mathbf{k})=k^2$.

The confinement of the 2DES is approximated by a triangular potential $V(z)=eFz$ and is taken into account by the

envelope functions $\phi_\uparrow(z)$ and $\phi_\downarrow(z)$ for the spin-up and spin-down conduction bands, respectively.

### B. The effective *g* factor

We solve the Schrödinger equation with the $2\times2$ Hamiltonian of Eq. (4.3) for the potential $V(z)=eFz$ and a magnetic field applied perpendicular to the 2DES. The energy dependence of the lowest Landau level for both spin orientations is calculated following Ref. 4. The resulting $g$ factor has a linear dependence on magnetic field:

$$g^*(B)=g^*(B=0)-cB(N+1/2). \tag{4.4}$$

The value of $c$ is determined by $a_{43}$, i.e., $c=8\langle a_{43}\rangle/B$. $\langle a_{43}\rangle$ is due to the isotropic $k$-dependent Zeeman contribution to the Hamiltonian. The angle brackets refer to an average over the extent of the wave function in the $z$ direction.

### C. ESR selection rules: Magnetic and electric dipole transitions

To investigate the processes responsible for the ESR we consider the single-electron Hamiltonian

$$H_0+H_{EDT}+H_{MDT}. \tag{4.5}$$

Here $H_0$ is the unperturbed single-electron Hamiltonian. The interaction with the electromagnetic field is given by

$$H_{EDT}=\mathbf{A}\cdot\mathbf{j} \tag{4.6}$$

for the electric dipole interaction and

$$H_{MDT}=g_0\mu_B\boldsymbol{\sigma}\cdot\mathbf{B}/2 \tag{4.7}$$

for the magnetic dipole interaction. $\mathbf{A}$ is the vector potential of the exciting electromagnetic wave and $\mathbf{B}=\boldsymbol{\nabla}\times\mathbf{A}$ its magnetic field. $\mu_B$ denotes the Bohr magneton and $g_0$ is the free electron Landé factor $(=2)$.

The ESR transition amplitudes are defined by the matrix elements of $\mathbf{H}_{EDT}$ and $\mathbf{H}_{MDT}$. Both EDT and MDT require a CRI polarization (opposite to that of the cyclotron resonance) for the spin-up to spin-down transition. This yields for the EDT

$$\begin{aligned}\langle f\downarrow|\mathbf{j}\cdot\mathbf{A}_{CRI}|i\uparrow\rangle/eA_0 &= \frac{P^2}{3\hbar}\Bigg\{\int\phi_f^*\frac{1}{i}\frac{\partial}{\partial z}\phi_i dz\left(-\frac{1}{E_i+E_g}+\frac{1}{E_i+\Delta+E_g}\right)\\ &+\int\left(\frac{1}{i}\frac{\partial}{\partial z}\phi_f\right)^*\phi_i dz\left(\frac{1}{E_f+E_g}-\frac{1}{E_f+\Delta+E_g}\right)\Bigg\}\\ &+\frac{\sqrt{6}PiC_2\epsilon_{xy}}{9\hbar}\Bigg\{\int\phi_f^*\phi_i dz\left(\frac{1}{E_i+E_g}-\frac{1}{E_i+\Delta+E_g}\right.\\ &\left.-\frac{1}{E_f+E_g}+\frac{1}{E_f+\Delta+E_g}\right)\Bigg\},\end{aligned} \tag{4.8}$$

and for the MDT

$$\langle f\downarrow|g_0\frac{\mu_B}{2}\boldsymbol{\sigma}\cdot\mathbf{B}_{CRI}|i\uparrow\rangle/eA_0=\frac{g_0\hbar}{4m_0}\frac{\sqrt{\epsilon}\,\omega_{ESR}}{c}\int\phi_f^*\phi_i dz. \tag{4.9}$$

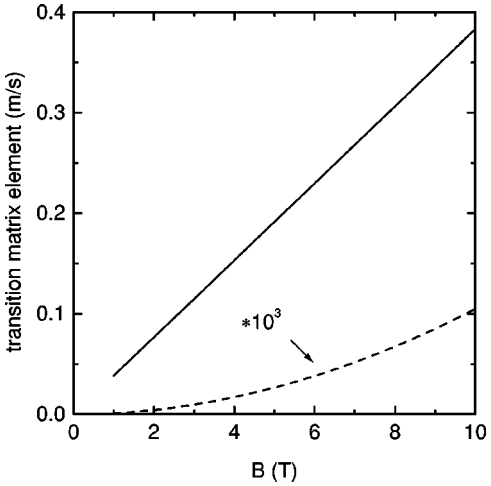


FIG. 7. Matrix elements for the magnetic (MDT) (solid) and electric-dipole transitions (EDT) (dashed) vs magnetic field $B$.

The first term in Eq. (4.8) originates from the $\mathbf{k}\cdot\mathbf{p}$ interaction as does the nonparabolicity of the conduction band. The second term is induced by strain $(\epsilon_{xy})$ and appears in crystals without inversion symmetry. Both terms depend on the spin-orbit splitting $\Delta$. $i\uparrow$ denotes the initial spin-up state and $f\downarrow$ the final spin-down state (notation for electrons in GaAs). $E_g$ is the energy gap, $E_i$ and $E_f$ are the energies of the initial and final states relative to the conduction band edge, $g_0$ and $m_0$ the free electron values of the Landé factor and the mass. $\epsilon$ is the dielectric constant, $A_0$ the MMW vector potential amplitude. The transition rate is thus approximately $\propto B^2$ (the static applied magnetic field) for the MDT. $\phi_f$ $(=\phi_\downarrow)$ and $\phi_i$ $(=\phi_\uparrow)$ are the envelope funtions in a triangular potential (due to the field $F$) given by the Airy function Ai[1]

$$\phi_{i,f}(z)\propto\mathrm{Ai}\left\{\left[\frac{2eFm^*(E_{i,f})}{\hbar^2}\right]^{1/3}\times\left[\frac{\pm g^*\mu_B B/2+\hbar\omega_c/2-E_{i,f}}{eF}+z\right]\right\}. \tag{4.10}$$

The energies $E_{i,f}$ are determined by the first zeros of Ai. The two envelope functions $\phi_i$ and $\phi_f$ differ only slightly because of the small change of $m^*$ between $E_i$ and $E_f$. The integral in Eq. (4.9) is therefore very close to unity.

## V. DISCUSSION

In the first part of the discussion we show that the ESR is a magnetic dipole transition and that single-electron transition energies are observed. Nevertheless, we can conclude from the temperature dependence of the ESR strength that the ground state of the 2DES at our lowest temperatures is a many-particle state with reduced spin polarization.

The experiments in standing waves clearly demonstrate that the ESR is a magnetic dipole transition (MDT). This is confirmed by the theoretical results using Eqs. (4.8) and (4.9). Figure 7 shows the calculated matrix elements of the MDT and of the EDT as a function of the magnetic field. The values used for the calculation are: $E_g=1.519$ eV, $P=10.49$ eV Å, $\Delta=0.171$ eV, $\epsilon=13.1$.[19] $F$ is assumed to be

$1.4\times10^4$ V/cm corresponding to a total 2D charge density of $10^{11}$ cm$^{-2}$. The zero-field values used for the effective Landé factor and mass are: $g^*=-0.44$, $m^*=0.067m_0$. As an example, at the resonance position of Fig. 6 (7.7 T) the ratio of the oscillator strengths MDT/EDT is $25\times10^6$. As a consequence the absorption process of the ESR is overwhelmingly a MDT since we can exclude a strong strain enhancement of the EDT [see the second term of Eq. (4.8)] to dominate. Such a strain can be caused by the lattice mismatch between the $Al_xGa_{1-x}As$ and the GaAs. This mismatch, however, is very small (of the order of 0.04%) and predominantly taken up by the thin pseudomorphic $Al_xGa_{1-x}As$ layer due to the large thickness ratio (0.5 mm GaAs, 78 nm $Al_xGa_{1-x}As$). Therefore, the strain in the GaAs is very small ($\approx4\times10^{-8}$). Furthermore, the growth direction of the sample is [001]. For this direction there are no off-diagonal strain components ($\epsilon_{xy}=\epsilon_{yz}=\epsilon_{zx}=0$). EDT terms containing the deformation potential $C_2$ can therefore be neglected.

The observed dependence of the magnetic field positions of the ESR on the MMW frequency yields the $g$-factor dependence shown in Fig. 3. These magnetic-field dependences are in excellent agreement with the theoretical results according to Eq. (4.4) and Ref. 4. Thus, the single-electron theory describes the experimental data exactly, i.e., Kohn's theorem is not violated. Notably, this agreement holds in the range of fractional filling factors and at temperatures where many-body effects start to play a role (weak $\nu=2/3$ FQHE minimum between 1.3 and 1.6 K, strong at 0.3 K). Even so, evidence for a many-particle ground state is found in the temperature dependence of the *strength* of the ESR as shown below.

For the discussion of the temperature dependence of the ESR signal the behavior of the nonresonant background is of importance. As can be seen from Fig. 4 the background signal strongly increases with decreasing temperature demonstrating an increasing sensitivity of the 2DES. Therefore, the reduction and disappearence of the ESR in the photoconductivity is not due to a general reduction of the sensitivity of $R_{xx}$ to the MMW absorption. Also the ESR matrix elements should not be temperature dependent since the single-electron wave functions are temperature independent. This leaves a change of the spin admixtures to the 2DES ground state as the basis for the interpretation of the temperature dependence: The gradual disappearence of the ESR signal between 1.6 and 0.3 K reflects equal strengths of the stimulated absorption and emission transitions (which add up to the net absorption). The former one corresponds to a spin-up to spin-down transition, the latter one to the opposite transition. The disappearence of the total absorption therefore indicates equal contributions of the two spins to the ground state, i.e. a vanishing of the spin polarization. Similar observations were made by Manfra *et al.*[13] where the strength of interband transitions into the two spin states were measured for varying filling factor. The relative strengths of the two transitions were interpreted in terms of the spin polarization. At $T=1.5$ K and filling factors around 0.8 the spin polarization was only about one third of that one for the independent-electron case.

A vanishing of the spin polarization can be caused by electron-electron interaction. A temperature dependence of the spin polarization in a comparable temperature range was predicted in finite-size studies for $\nu=2/3$,[10] and for a range of filling factors below $\nu=1$.[11] For $g$-factors $\approx0.4$ the following behavior was predicted: At high temperatures, $kT\geqslant\hbar\omega_{ESR}$, the spin polarization is destroyed by thermal excitation of single electrons across the spin gap. It increases towards intermediate temperatures as the low-lying excited many-body states are spin polarized and vanishes again at lower temperatures when $kT/(e^2/4\pi\epsilon\epsilon_0 l_c)<0.01$ ($T<1.6$ K at 10 T) where the spin unpolarized ground state dominates. Along these lines we interpret our results at 1.6 K and below as a transition from the intermediate (with spin polarization) to the low-temperature range (no spin polarization).

The second part of the discussion concerns the detection of the ESR in transmission and photoconductivity and the ESR line shape.

In previous and present experiments it has not been possible to detect the ESR of electrons in $Al_xGa_{1-x}As$/GaAs in a transmission or cavity experiment. The crucial point within this context is the strength of the transition-matrix element. On the basis of our theoretical and experimental findings it can be calculated and an estimate of the change of the transmission at the ESR be given. For this purpose, we compare the matrix elements of the ESR with that of the cyclotron resonance (CR). Using Eq. (4.9) for the ESR (with $\int\phi_f^*\phi_i dz=1$) and

$$\frac{\hbar n_r}{l_c m_0} \tag{5.1}$$

for the CR matrix element the ESR/CR ratio is given by

$$\frac{g_0 l_c \omega_{ESR}}{4c}, \tag{5.2}$$

where $n_r=\sqrt{\epsilon}$ is the refractive index, $l_c$ is the magnetic length. For electrons in $Al_xGa_{1-x}As$/GaAs the ratio is $4\times10^{-6}$ at $B=8$ T.

In an actual measurement interference effects of the sample surfaces have to be taken into account. For the CR this was done classically by Kennedy *et al.*[20] Using the definitions $\Omega=n_s e^2\tau/m\epsilon_0 c=\sigma_0/\epsilon_0 c$ ($\sigma_0$ is the dc conductivity at $B=0$), $X_\pm=1+(\omega_c\pm\omega)^2\tau^2$, $\theta=n_r d\omega/c$ ($d$ is the sample thickness), $\Omega_1=(4+\Omega)\Omega$, $\Omega_2=(2+n_r^2+\Omega)\Omega$, the power transmissions for the two circular polarizations are given by

$$T_\mp=2X_\pm/\{\cos^2\theta(4X_\pm+\Omega_1)+n_r^{-2}\sin^2\theta[(1+n_r)^2X_\pm+\Omega_2]-n_r^{-1}\cos\theta\sin\theta(n_r^2-1)2\Omega(\omega-\omega_c)\tau\}. \tag{5.3}$$

For a linearly polarized wave the transmission is then given by $T=\frac{1}{2}(T_+ + T_-)$. For $n_s=1.4\times10^{11}$ cm$^{-2}$, $\tau=30$ ps, and $n_r=3.6$ for GaAs, at 8 T the transmission at the CR minimum is calculated to be near 50% of the $B=0$ value (corresponding to almost 100% absorption in the CRA polarization), a typical experimental situation. In comparison, for the ESR, $\Omega$ has to be modified by the ESR/CR ratio of the oscillator strengths:

$$\Omega_{ESR}=\Omega_{CR}\left(\frac{g_0 l_c \omega_{ESR}}{4c}\right)^2. \tag{5.4}$$

$\tau$ is set to 1 ns to reproduce the observed linewidths in our photoconductivity experiments. $\omega_c$ is replaced by $\omega_{ESR}$ in $X_\pm$. In this case the relative change in transmission is of the order of $10^{-5}$. This low value is most likely the reason why it has not yet been possible to observe the ESR in a transmission experiment. Indications of an ESR absorption have been observed in a high-$Q$ ($\sim$1000) cavity experiment, however, these results were not reproducible.[21] Reproducible observations of the ESR have been achieved only in bulk $n$-GaAs.[22] An important difference between the bulk and the 2D samples is the number of available spins. In our 2D sample ($3\times7$ mm$^2$) there are about $3\times10^{10}$ spins in the 2DES. A bulk sample ($3\times7\times0.5$ mm$^3$) with a carrier density of $10^{15}$ cm$^{-3}$ has $10^{13}$ available spins.[22] A corresponding multilayer 2DES sample would require 300 layers and would show an ESR transmission dip of about $1.5\times10^{-3}$. The detectability would strongly depend on the homogeneity of the layers.

It is interesting to note that the value of $\tau$ (1 ns) used to reproduce the line width of our photoconductivity experiment agrees with the spin-flip time deduced from the scattering rate of hot electrons.[23] In that experiment quantum point contacts were used to inject hot electrons into the upper spin level and to detect the scattering into the lower one. This relaxation mechanism is equivalent to the mechanism determining the lifetime in the upper spin level of the ESR experiment and therefore the width of the resonance transition. From the agreement of the two values we conclude that there is no additional mechanism broadening the resonance in the photoconductivity experiment (see also the discusssion on the Overhauser effect and the line width below).

Any discussion of the strength of the ESR in photoconductivity must also include mechanisms producing the change in the resistance $R_{xx}$. As stated above the observed ESR energies correspond to single-electron transitions. For an estimation of an upper limit of $\Delta R_{xx}$ we consider single-electron transitions with the initial and final states of the ESR being the $0\uparrow$ and $0\downarrow$ states, respectively. With a different mobility in the final state a $\Delta R_{xx}$ signal can be observed if the nonequilibrium population of the state is large enough. To calculate this nonequilibrium population we assume a lifetime of 1 ns (as for the transmission calculation), a photon flux of $1.8\times10^{20}$ s$^{-1}$ (corresponding to the 5 mW used in the experiment) and the absorption efficiency of $10^{-5}$ (see above). We arrive at about $2\times10^6$ spins redistributed, a relative change of about $7\times10^{-5}$ ($\Delta R_{xx}\approx10^{-4}-10^{-3}$ in the experiment). Therefore, even a strong difference in the electron mobilities of the initial and final states would cause only a very small change in $\Delta R_{xx}$. The most pronounced effect would be due to transitions from localized to delocalized states or vice versa. As a second mechanism, we consider a change of the electron distribution and an increase of the average energy (electron heating) within the density of states of the lowest spin Landau level. It is assumed to produce our nonresonant background signal via MMW absorption within this level. This mechanism can also cause the ESR signal where after the resonant absorption relaxing electrons transfer energy and produce the increase of the average energy. In both cases (resonant and nonresonant) the MMW absorption is expected to have a similar effect on the resistance, including the sign of $\Delta R_{xx}$. This expectation is met by the experimental observations. The interpretation is further supported by the observation that $\Delta R_{xx}$ has the same sign as $\Delta R_{xx}^T$ produced by an increase of the lattice temperature.

A dependence of the shape and position of the ESR on the direction of the magnetic field sweep was found in previous work.[16,17] This was attributed to the Overhauser effect where a coupling of the electronic and nuclear spins occurs. Via this coupling nuclear spins become polarized. The relaxation of the nuclear spins was found to be extremely slow (relaxation times up to $10^3$ s) within the $R_{xx}$ minima near integer filling factors.[17,12] Consequently a stationary nonequilibrium nuclear spin polarization can be built up. The associated magnetic moments then cause an internal magnetic field shifting the applied magnetic field necessary for the ESR to lower values. Therefore, for a decreasing applied magnetic field the electrons remain in the ESR condition as the nuclear spin polarization builds up. Comparing the ESR signal trace with that of a rising magnetic field, it is broadened and shifted downwards. As shown in Fig. 5 no such shifts and changes in shape are observed in our experiments. At the temperatures and filling factors where we observe the ESR, the nuclear relaxation times are short (20–60 s) compared to $\nu=1$.[12] Therefore, the stationary nonequilibrium nuclear spin polarization is small. Furthermore, the MMW power used in our experiment is one to two orders of magnitude lower than in Refs. 3 and 17. Both the short relaxation time and the low MMW power contribute to the lack of the Overhauser effect in our data. This also adds a further point to the discussion of the ESR linewidth. Above, we have found an indication that there is no additional broadening beside the lifetime broadening. A broadening could be due to the Overhauser effect, which we rule out for our experimental conditions. Another source of broadening could be inhomogeneous strain. However, as shown above for a (001) layer the strain-induced matrix element vanishes.

## VI. SUMMARY

In this paper we have studied the ESR of the 2DES in $Al_xGa_{1-x}As/GaAs$ by a millimeter wave photoconductivity technique. The results concern the transition selection rules and matrix elements, the photoconductivity mechanism, the magnetic-field dependence of the effective $g$ factor, the ESR linewidth, and the spin polarization in the lowest Landau level.

The mechanism which causes the change of the resistance is shown to be an increase of the average energy of the 2DES after the single-electron ESR transition and subsequent relaxation. The experiments which separate the electric and magnetic components of the millimeter waves by exploiting a standing wave pattern, show, supported by theoretical calculations, that in the 2DES of $Al_xGa_{1-x}As/GaAs$ heterostructures the ESR is dominated by magnetic dipole transitions. The ESR linewidth is determined by the lifetime in the upper spin state, which is of the order of 1ns.

Our ESR experiments have been performed in the temperature and Landau level filling ranges where FQHE features occur in $R_{xx}(B)$. Although many-body effects are gen-

erally assumed to be responsible for the occurence of the FQHE no indication of their influence on the ESR transition energy has been detected. The magnetic-field dependence of the transition energy and of the effective $g$ factor can be exactly reproduced using a $\mathbf{k}\cdot\mathbf{p}$ perturbation calculation for noninteracting electrons. This shows that no violation of Kohn's theorem occurs. Despite the lack of evidence for electron-electron interactions in the ESR transition energies, the interactions are effective via an admixture of spin-up and spin-down contributions to the many-particle ground state of the 2DES. This causes the disappearence of the ESR signal with decreasing temperature. The temperature dependence is in accordance with predictions of finite size studies,[10,11] *viz.* the transition from a spin-polarized state to a state with strongly reduced spin polarization.

## ACKNOWLEDGMENTS

This work was supported by the European Union (TMR Contract No. FMRX-CT98-0180) and the Fonds zur Förderung der wissenschaftlichen Forschung, Austria (Project No. P12024-PHY). The supply of $Al_xGa_{1-x}As$/GaAs samples, grown by MBE at the Deutsche Telekom, Darmstadt, is particularly acknowledged.

[1] T. Ando, A.B. Fowler, and F. Stern, Rev. Mod. Phys. **54**, 437 (1982).
[2] D. Stein, K. v. Klitzing, and G. Weimann, Phys. Rev. Lett. **51**, 130 (1983).
[3] M. Dobers, K. v. Klitzing, and G. Weimann, Phys. Rev. B **38**, 5453 (1988).
[4] G. Lommer, F. Malcher, and U. Rössler, Phys. Rev. B **32**, 6965 (1985).
[5] E. Abrahams, Physica E **3**, 69 (1998).
[6] R.B. Laughlin, Phys. Rev. Lett. **50**, 1395 (1983).
[7] J.K. Jain, Phys. Rev. Lett. **63**, 199 (1989).
[8] B.I. Halperin, P.A. Lee, and N. Read, Phys. Rev. B **47**, 7312 (1993).
[9] P.A. Maksym, J. Phys.: Condens. Matter **1**, 6299 (1989).
[10] T. Chakraborty and P. Pietiläinen, Phys. Rev. Lett. **76**, 4018 (1996).
[11] T. Chakraborty, P. Pietiläinen, and R. Shankar, Europhys. Lett. **38**, 141 (1997).
[12] S.E. Barrett, G. Dabbagh, L.N. Pfeiffer, K.W. West, and Z. Tycko, Phys. Rev. Lett. **74**, 5112 (1995).
[13] M.J. Manfra, E.H. Aifer, B.B. Goldberg, D.A. Broido, L. Pfeiffer, and K. West, Phys. Rev. B **54**, R17 327 (1996).
[14] W. Kohn, Phys. Rev. **123**, 1242 (1961).
[15] R. Meisels, I. Kulac, G. Sundaram, F. Kuchar, B.D. McCombe, G. Weimann, and W. Schlapp, Surf. Sci. **361/362**, 55 (1996).
[16] M. Dobers, K. v. Klitzing, J. Schneider, G. Weimann, and K. Ploog, Phys. Rev. Lett. **61**, 1650 (1988).
[17] A. Berg, M. Dobers, R.R. Gerhardts, and K. v. Klitzing, Phys. Rev. Lett. **64**, 2563 (1990).
[18] H.-R. Trebin, U. Rössler, and R. Ranvaud, Phys. Rev. B **20**, 686 (1979).
[19] H. Mayer and U. Rössler, in High Magnetic Fields in Semiconductor Physics III, edited by G. Landwehr, Springer Series in Solid State Science Vol. 101, (Springer, Berlin, 1992), p. 589.
[20] A. Kennedy, R.J. Wagner, B.D. McCombe, and J.J. Quinn, Solid State Commun. **18**, 275 (1976). Equation (7) of this reference contains an error: the term $(n_a+n_0-n_an_0+n_{Si}^2)$ which reduces to $(1+n_r^2)$ (with $n_a=n_0=1$, $n_{Si}=n_r$ for our case) produces an unphysical oscillatory behavior with respect to the sample thickness, even if $n_r=1$. The oscillatory behavior vanishes when using the correct term $(n_r^2-1)$ instead.
[21] M. Seck, Ph.D. thesis, University of Konstanz, Germany, 1996.
[22] M. Seck, M. Potemski, and P. Wyder, Phys. Rev. B **56**, 7422 (1997).
[23] B.W. Alphenaar, H.O. Müller, and K. Tsukagoshi, Phys. Rev. Lett. **81**, 5628 (1998).